

Secular Variations in the Production of Cosmogenic Isotopes in the Earth's Atmosphere

K. O'BRIEN

Environmental Measurements Laboratory, U.S. Department of Energy, New York, New York 10014

The dependence of cosmogenic isotope production on solar modulation and on geomagnetic field intensity has been calculated, and spallation yields based on the Silberberg-Tsao formalism have been determined. The stratospheric inventory of ^7Be during the period 1970–1974 has been calculated to be about 4.5 mCi, in good agreement with measured values. The calculated radiocarbon reservoir of $1.75 \text{ cm}_e^{-2} \text{ s}^{-1}$ (where results are integrated over the whole earth) is in good agreement with the experimental value of 1.8. Geomagnetic and solar effects were taken into account.

INTRODUCTION

Lal and Peters [1962] argue that the experimental data on nucleons and nuclear reactions in the earth's atmosphere are extensive enough and consistent enough to determine cosmogenic isotope production rates more accurately than can hadronic cascade calculations. Why then carry out such calculations? Three reasons are the following. First, an accurate calculation demonstrates a detailed understanding of the physical processes involved. Second, atmospheric cosmic rays are time dependent, and the experimental data are averages characteristic of a particular interval of time not necessarily extensible to other times or intervals of time. Third, the calculation can be extended to conditions which are not experimentally accessible, such as the remote past.

While Lal and Peters referred specifically only to Benioff's [1956] work, there have been a number of such cascade calculations both before and since [Hess *et al.*, 1961; Newkirk, 1963; Lingenfelter, 1963; Merker, 1970; Light *et al.*, 1973], stimulated chiefly by the need to understand the balance between the production of radiocarbon and the quantity of radiocarbon in its reservoirs, and the time dependence of the production rate.

This paper presents the results of a hadronic cascade calculation that was carried out for a range of solar modulation conditions and geomagnetic field strengths. In addition, a number of cosmogenic isotope yields were calculated by using both Rudstam's [1966] CDMD (charge distribution-mass distribution) method and Silberberg and Tsao's [1973a, b] method. The ^7Be inventory was calculated and compared with extensive measurements carried out during a 4½-year period. The agreement between calculation and measurement was about 10%. Radiocarbon production was also calculated and compared with the reservoir estimates of Grey [1972], Damon [1978], and Suess [1965]. Excellent agreement was found. The dependence of radiocarbon production on geomagnetic field strength was compared with Elsasser *et al.*'s [1956] model, and that on the mean annual sunspot number (the Wolf index) with Lingenfelter's [1963] model. Good agreement with both models was obtained.

DESCRIPTION OF THE TRANSPORT CALCULATION

Solar Modulation

The primary cosmic ray flux in the solar system at the earth's orbit is a mixture of energetic protons, alpha particles, and a small admixture of heavier nuclei which are omitted in

This paper is not subject to U.S. copyright. Published in 1979 by the American Geophysical Union.

this treatment. The flux and its composition vary over the 11-year solar activity cycle; thus to calculate cosmic ray phenomena as a function of time, the time-dependent cosmic ray spectra must be obtained.

It has been shown theoretically [Gleeson and Axford, 1967] that the effect on the galactic cosmic ray spectrum of passage through the interplanetary medium is approximately the same as would be produced by a heliocentric electrical potential with a magnitude at the earth's orbit equal to the energy lost by the cosmic rays while they are interacting with the solar wind. As solar activity waxes and wanes with the 11-year solar cycle, the energy lost by galactic cosmic rays in penetrating the interplanetary medium to the earth's orbit rises and falls with it. An increase in this potential causes a decline in the cosmic ray intensity at that point, while a decrease results in a corresponding rise. This approximation at cosmic ray energies above about 50 MeV appears to be a good one and has been used by Ehmert [1960], Freier and Waddington [1965, 1966], and Cleghorn *et al.* [1971]. The ground level counting rates of several cosmic ray neutron monitors have been related to the primary cosmic ray spectrum by means of these Ehmert potentials [O'Brien and Burke, 1973] and are shown in Table 1. Thus the spectra of protons and alpha particles at the earth's orbit can be computed from a knowledge of the appropriate ground level neutron monitor counting rate.

The spectra incident on the earth's atmosphere are determined [O'Brien and Burke, 1973] from

$$n(E) = n_0(T) \left[\frac{p(E)}{p(T)} \right]^2$$

$$T = E + ZU$$

$$p(x) = \frac{1}{c} \left(x^2 + 2Am_p c^2 x \right)^{1/2}$$

where m_p is the proton mass in MeV, n_0 is the unmodulated galactic spectrum of atomic weight A and atomic number Z $\text{sr}^{-1} \text{ cm}^{-2} \text{ s}^{-1} \text{ MeV}^{-1}$ having an energy of E MeV, and U is the Ehmert potential in megavolts.

For n_0 the unmodulated proton and alpha particle spectra of Freier and Waddington [1965, 1966] were used for energies below 10 GeV. For energies above 10 GeV the spectra of Pal [1967] and O'Brien [1972] were used.

While these spectra are not recent, it is not practical to replace them with later data: to preserve the relationship obtained earlier between Ehmert potential and counting rate, it was necessary to make these spectra integral to the computer

TABLE 1. Calculated Neutron Monitor Counting Rates* as a Function of Solar Modulation Expressed in Terms of the Ehmert Potential

Potential, MV	Deep River	Alert	Goose Bay	Inuvik
0	2.247×10^6	8.114×10^5	7.741×10^5	7.542×10^5
50	2.208×10^6	7.976×10^5	7.611×10^5	7.408×10^5
134	2.147×10^6	7.766×10^5	7.411×10^5	7.198×10^5
200	2.104×10^6	7.610×10^5	7.262×10^5	7.057×10^5
300	2.046×10^6	7.399×10^5	7.060×10^5	6.860×10^5
500	1.948×10^6	7.040×10^5	6.719×10^5	6.525×10^5
700	1.864×10^6	6.740×10^5	6.433×10^5	6.246×10^5
1000	1.769×10^6	6.377×10^5	6.087×10^5	5.905×10^5

*Counting rates are in counts per hour.

code. It is felt that these spectra are accurate enough for the purpose of these calculations.

Atmospheric Cosmic Ray Propagation

The behavior of cosmic rays in the earth's atmosphere, averaged over time, is governed by the stationary form of the Boltzmann equation:

$$B_q \Phi_q(r, E, \Omega) = S_{qj}$$

$$B_q = \Omega \cdot \nabla + \sigma_q + \frac{C_q}{P_q r} - \frac{\partial}{\partial E} k_q$$

$$S_{qj} = \int_{4\pi} d\Omega \int_E^\infty dE_B \sigma_{qj} F_{qj}(E_B \rightarrow E, \Omega' \cdot \Omega) \Phi_j(r, E_B, \Omega')$$

$$C_q = m_q H / c \tau_q$$

where

- B_q Boltzmann operator for a q type particle;
- S_{qj} scattering-down integral describing the production of q type particles from j type particles due to collisions at higher energies;
- C_q governs the loss of q type particles to decay processes;
- r depth in the atmosphere in grams per square centimeter;
- E kinetic energy of the particle in MeV;
- Ω unit vector in the direction of particle travel;
- Φ_q q type particle flux per MeV per second per steradian at depth r having a direction Ω ;
- σ_q total cross section for the absorption of a q type particle in square centimeters per gram;
- k_q stopping power of a charged q type particle in air in MeV cm²/g;
- σ_{qj} cross section for the production of q type particles from collisions with, or decay by, j type particles in square centimeters per gram;
- F_{qj} number of q type particles per second per steradian at E and Ω' ;
- m_q rest mass of a q type particle in MeV/c²;
- P_q momentum of a q type particle in MeV/c;
- τ_q mean life of a q type particle in its rest frame in seconds;
- H scale height of the earth's atmosphere (taken as 6.2×10^5 cm); and
- c velocity of light (3×10^{10} cm/s).

It is understood that k_q is zero for neutrons, neutral pions, and photons; S_{qj} is zero for muon scattering; and C_q is zero for stable particles (protons, photons, etc.).

As the energy of the incoming particles is above 100 MeV, the cross sections used were geometric and constant with en-

ergy [Barashenkov *et al.*, 1968]. The stopping powers were taken from O'Brien [1972]. The production spectra were derived from a combination of experimental and theoretical models [O'Brien, 1971, 1975].

The Boltzmann equation was solved by using a straight-ahead code based on the work of Passow [1962]. This program transports neutrons, protons, and pions. The protons and neutrons in the incident primary cosmic ray α particle flux are treated as unbound after entering the earth's atmosphere. (While they are interacting with the solar wind and with the earth's geomagnetic field, α particles are treated as bound.) In dilute media such as the atmosphere, kaons which are produced in nuclear interactions generally decay before undergoing a nuclear collision. For this reason, kaon production was accounted for, but kaon transport was ignored. The program gives good agreement with cosmic ray pion, proton, neutron, and muon spectra [O'Brien, 1971, 1975a, b].

For this calculation the atmosphere was modeled as a spherical shell with an inner radius of 6.371×10^8 cm, a thickness of approximately 40 km, and an exponentially distributed density corresponding to a scale height of 6.2 km. (The scale height is the ratio of the atmospheric depth to the density at that depth.)

The Geomagnetic Field

The magnetic rigidity of cosmic ray particles is defined as $r = pc/q$, where p and q are the momentum and charge of the particle and c is the velocity of light. The magnetic field of the earth deflects incoming cosmic rays depending on their rigidity and angle of incidence. For each angle of incidence there is a critical rigidity below which the incoming particle cannot interact with the earth's atmosphere. The cutoff fields (the cutoff being the critical rigidity) for the calculations described in this study were calculated with the aid of the computer code Angri [Bland and Cioni, 1968].

The computational approach described so far will yield cosmic ray energy spectra in the earth's atmosphere as a function of solar modulation and altitude at one location characterized by the geomagnetic field. To determine worldwide production, it is necessary to integrate over the whole globe. To do this, the vertical cutoff rigidity parameter which ranges from zero to 17.5 GV [Shea and Smart, 1967] was divided into 36 equal intervals. Calculations were performed at each of these intervals, integrated vertically down through the atmosphere to either the earth's surface or the tropopause, grouped by geomagnetic latitude, and then summed over the globe.

Archaeomagnetic data indicate that the earth's magnetic field has varied approximately sinusoidally over the past 9000 years from 0.5 times the current value about 6000 years ago to about 1.5 times the present value about 2000 years ago [Cox,

1969; Bucha, 1969; Bucha, 1970; Kitazawa, 1970]. There is evidence from excavations in the Lake Mungo area of south-eastern Australia that between 25,000 and 35,000 years ago the geomagnetic field may have reached 3 times its current value during a geomagnetic excursion [Barbetti, 1976]. To simulate the effect of a change in the earth's magnetic field strength by some factor M , the vertical cutoff rigidity was multiplied by M before calculating the cosmic ray fluxes in the earth's atmosphere and integrating over the globe.

The justification for this treatment is that a charged particle describing a fixed curved path in a magnetic field (above the earth's atmosphere, let us say) must have a rigidity proportional to the magnetic field strength.

Cosmogenic Isotope Calculations

The most convenient approach is to calculate the concentration of high-energy inelastic collisions (called 'stars' because of their appearance in a photographic plate) in the air and determine the spallation yield per star of a particular isotope separately. There is some sacrifice of accuracy in not calculating each produced nuclide separately, since the isotope production cross sections are energy dependent and since the hadron spectra involved change slightly in shape with changes in altitude, latitude, solar modulation, and so forth. At the top of the atmosphere, of course, the proton spectrum (and the primary alpha particle spectrum) is discontinuous in energy at each zenith and azimuth owing to the effect of the cutoff field.

The computational advantage gained by this approximation is enormous and well worth it. New yields or revised yields can easily be applied to the same body of computed data. The volume of calculations is very much reduced, and the applicability of the results is considerably broadened.

This procedure cannot be applied to the production of radiocarbon. Most radiocarbon production is the result of the thermal and resonance capture of neutrons by nitrogen, along with some production by spallation at higher energies. However, the mathematical approximations used to obtain a solution to the Boltzmann equation applicable to high-energy hadrons fail below 100 MeV [O'Brien, 1971]. This low-energy limit has no effect on charged atmospheric cosmic ray transport because of charged particle stopping which limits the number of these particles at low energies. Neutrons, however, are uncharged and extend all the way down to thermal energies. In order to account for radiocarbon production below 100 MeV the low-energy spectrum has been assumed to have the same shape as the spectrum reported by Hess *et al.* [1961]. This is essentially the same as the spectrum which was obtained by O'Brien *et al.* [1978], but which was not available until this study was nearly complete.

This necessitates the assumption that there is no change in the shape of the neutron spectrum below 100 MeV with altitude, modulation, and changes in geomagnetism. This assumption is a reasonable one. All atmospheric neutrons are secondaries resulting from collisions between the primary cosmic rays and the constituents of the atmosphere. Hence they reflect the behavior of the primary spectra, production mechanisms, and atmospheric absorption cross sections. The shape of the energy spectra of protons and neutrons above 100 MeV is essentially independent of these factors, so that the low-energy production of neutrons from high-energy collisions and the resulting spectra, when they are not too close to a boundary, will follow suit. At the very top of the atmosphere some diffusion-hardening will take place that will not be reflected in this treatment; a small overestimate will result in the flux

calculated by the method used in this paper [O'Brien, 1971] within a few grams per square centimeter of the top.

The fact that the expected invariance of low-energy neutron spectral shape with altitude is clearly evident in the measurements of Hess *et al.* [1961] and the calculations of Armstrong *et al.* [1973] justifies the adequacy of this assumption.

Scope of the Transport Calculations

Radiocarbon and star production have been calculated as a function of altitude in the earth's atmosphere and geomagnetic latitude and have been integrated over the total atmosphere for solar modulation conditions ranging from a Deep River neutron monitor hourly counting rate of 2.247×10^6 (no modulation) to one of 1.769×10^6 (strongly modulated). The earth's magnetic field was varied from zero to 5 times the current magnetic field strength ($0 \leq M \leq 5$). The production rate in the stratosphere alone was also obtained for the full range of modulation conditions but only for the current geomagnetic field strength ($M = 1$).

DESCRIPTION OF THE RESULTS

By using the four sets of proton and alpha particle spectra of Figure 1, which range from unmodulated to strongly modulated, star densities and radiocarbon production rates were calculated for $M = 0, 0.5, 1, 1.5,$ and 5 . The values of the star density obtained as a function of altitude and latitude are shown in Figure 2. The results for star and radiocarbon production integrated over the whole earth are summarized in Tables 2 and 3. Under conditions typical of today (vide infra), $U = 200$ MV and $M = 1$, about 60% of the radiocarbon production and about 70% of the star production take place in the stratosphere. These results agree rather nicely with those of Lal and Peters [1962], as shown in Table 4.

The effect on the radiocarbon inventory of the time dependence of solar activity and the variations of the earth's atmosphere will be discussed at greater length later on.

Spallation Yields

The yield, per star, of some cosmogenic isotope x is defined to be

$$y_x = \frac{\int_a^\infty \sigma_x(E) \Phi_i(E) dE}{\int_a^\infty \sigma_{\text{nonel}}(E) \Phi_i(E) dE}$$

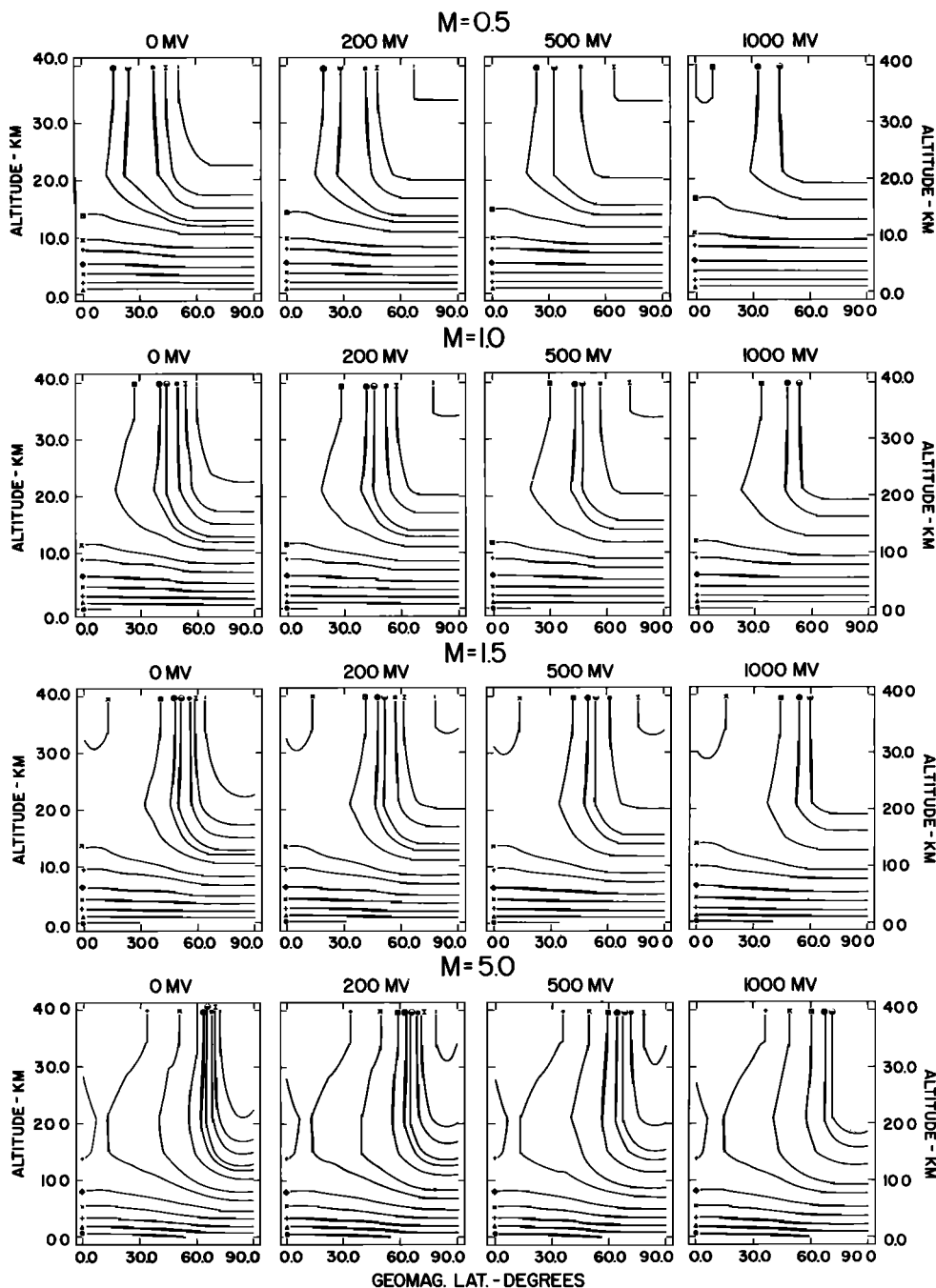
where $\sigma_x(E)$ is the cross section for the production of x as a function of energy, $\Phi_i(E)$ is the hadron energy spectrum ($i = n, p, \pi^\pm$), $\sigma_{\text{nonel}}(E)$ is the total nonelastic cross section, and a is the lower-energy limit of the calculation (100 MeV).

The major contributors to y_x , namely, the neutron and proton spectra, tend to reflect the behavior with energy of the primary nucleon spectrum and show relatively little change of shape with changing conditions of altitude, latitude, or modulation. The pion spectrum, which does change drastically with altitude, contributes less than 5% to the total yield. Hence it is assumed that the spallation yield y_x is constant everywhere. To calculate it, hadron spectra are chosen from conditions corresponding to the mean global production rate: at 45° geomagnetic latitude, at an altitude of 10 km, $U = 200$ MV, and $M = 1$.

Both Rudstam's [1966] CDMD method and Silberberg and Tsao's [1973a, b] method were used. The composition of the atmosphere was taken from Kallmann-Bijl *et al.* [1961]. The results for both models are summarized in Table 5.

The study of *Yasyulis et al.* [1974] indicates that the error in assuming γ_x constant everywhere is of the order of 10%. Spectral and atmospheric compositional differences may result in differences amounting to a factor of 2.

The ratios of the two sets of results, those of Rudstam and those of Silberberg and Tsao, are consistent with the generally accepted view that the Rudstam method has a coefficient of variation amounting to about 300 and that the Silberberg-



15 CONTOUR LEVELS - STARS/(g-s)

- | | | |
|--------------|--------------|--------------|
| ■ .10000E-05 | ◆ .30000E-03 | ● .10000E-01 |
| ● .30000E-05 | + .10000E-02 | * .10000E-01 |
| ▲ .10000E-04 | x .20000E-02 | ⌘ 20000E-01 |
| + .30000E-04 | ■ .50000E-02 | .30000E-01 |
| x .10000E-03 | ● .80000E-02 | ★ 50000E-01 |

Fig. 1. Star density contours in the earth's atmosphere as a function of the earth's geomagnetic field strength, in multiples of its current value (rows) and as a function of solar modulation expressed in terms of the Ehmer potential in megavolts (columns).

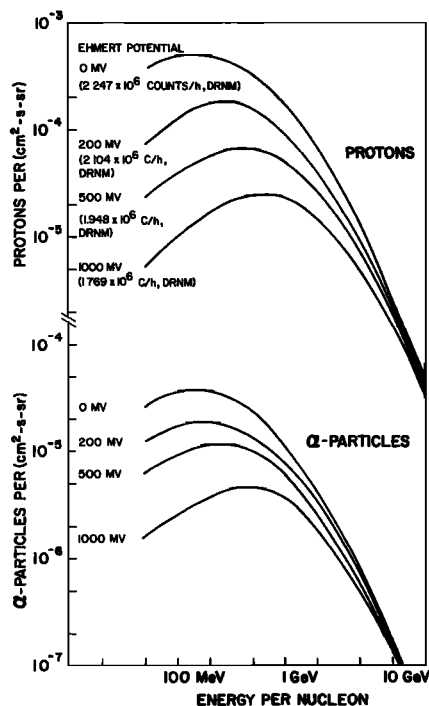


Fig. 2. Cosmic ray σ and proton spectra incident on the earth's atmosphere for various modulation conditions.

Tsao approach has a coefficient of variation of 20–30. Hereafter, 'calculated yields' will refer to yields obtained by the Silberberg-Tsao procedure.

Experimental Yields

Lal and Peters [1967] have published a number of spallation yields, some of which are based on experimental data. In addition, Young *et al.* [1970] have published isotope production rates in argon measured at an altitude of about 20 km near 50° geomagnetic latitude (with a vertical cutoff of about 2.5 GV). Combining these data with the calculated star production rates allows the inference of the corresponding spallation yields. Experimental yields from both sources are exhibited in Table 6.

I have not been able to find a quantitative assessment of the total experimental error in either paper, but the results as expressed in Table 6 are consistent with apportioning 30% equally to measurement and to calculation.

ISOTOPIC INVENTORIES

Beryllium 7

Aircraft and balloon measurements of ${}^7\text{Be}$ in the stratosphere carried out under the direction of the Health and Safety

Laboratory (now the Environmental Measurements Laboratory) from 1970 to 1974 (M. Schonberg, unpublished data, 1977) are shown in Figure 3. The time-dependent ${}^7\text{Be}$ inventory was calculated by using the Silberberg-Tsao spallation yield of Table 5 along with the stratospheric star density totals of Table 2 to construct an array of ${}^7\text{Be}$ inventories versus Ehmert potentials. Deep River neutron monitor data [Steljes, 1973; Wilson and Bercovitch, 1975] were then used to obtain the modulation corresponding to each measurement period and hence the ${}^7\text{Be}$ production rate. To pass from isotope production to radioactivity, a half-residence time of 10 months was assumed [Krey and Krajewski, 1970], and the equilibrium of decay and production was assumed. Thus

$$I(t) = 138y_{\text{Be-7}}S(t) \left[\frac{\lambda_d}{\lambda_R + \lambda_d} \right]$$

$$\lambda_i = \ln 2/H_i \quad i = R, d$$

where

- $I(t)$ time-dependent inventory in megacuries, the constant 138 converts from radiocarbon atoms in units of $\text{cm}_e^{-2} \text{s}^{-1}$ to megacuries (where subscript e signifies that results are integrated over the whole earth);
- $y_{\text{Be-7}}$ yield (from Table 5);
- $S(t)$ time-dependent worldwide star production rate for the stratosphere (Table 2);
- λ_i removal rate for radioactive decay or stratospheric residence;
- H_i half period for radioactive decay or stratospheric residence;
- R corresponds to residence time;
- d corresponds to radioactive decay.

Overall agreement is seen to be very good. The time dependence is correctly given.

Radiocarbon

Long-term variations. Elsasser *et al.* [1956] derived a relationship between the earth's magnetic field strength and radiocarbon production which is $Q \propto M^{-0.82}$, where Q is the production rate and M is the geomagnetic dipole moment in units of the current value, i.e., with today's field strength taken as unity. Plotting the data from Table 3 on Figure 4, it can be seen that this formula describes the radiocarbon production dependence on M over all conditions of modulation for M as high as 5. Not unexpectedly, as Figure 5 shows, the Elsasser, Ney, and Winckler formula applies equally well to spallation-produced isotopes.

In order to account for the effect on the total accumulated value of radiocarbon of the previously mentioned sinusoidal

TABLE 2. Star Production Rate*

Ehmert Potential, MV	Deep River Neutron Monitor Counting Rate, counts/h	Multiple of Current Geomagnetic Field Strength					Stratosphere, $M = 1.0$
		Total Atmosphere					
		$M = 0$	$M = 0.5$	$M = 1.0$	$M = 1.5$	$M = 5$	
0	2.247×10^6	5.049	2.825	2.087	1.713	0.9412	1.522
200	2.104×10^6	3.922	2.462	1.855	1.535	0.8417	1.315
500	1.948×10^6	3.008	2.108	1.630	1.363	0.7658	1.108
1000	1.769×10^6	2.225	1.746	1.395	1.177	0.6864	0.9227

*Star production rate is in units of $\text{cm}_e^{-2} \text{s}^{-1}$, where subscript e signifies that results are integrated over the whole earth.

TABLE 3. Radiocarbon Production Rate*

Ehmer Potential, MV	Deep River Neutron Monitor Counting Rate, counts/h	Multiple of Current Geomagnetic Field Strength					Stratosphere, <i>M</i> = 1.0
		Total Atmosphere					
		<i>M</i> = 0	<i>M</i> = 0.5	<i>M</i> = 1.0	<i>M</i> = 1.5	<i>M</i> = 5	
0	2.247 × 10 ⁶	4.979	2.781	2.075	1.713	0.9374	1.303
200	2.104 × 10 ⁶	3.828	2.426	1.831	1.534	0.8448	1.116
500	1.948 × 10 ⁶	2.937	2.087	1.631	1.367	0.7680	0.9394
1000	1.769 × 10 ⁶	2.188	1.738	1.404	1.191	0.5821	9.7817

*Radiocarbon production rate is in units of cm_e⁻² s⁻¹, where subscript e signifies that results are integrated over the whole earth.

9000-year change in magnetic field strength, *Ralph's* [1973] approach is followed.

Let

$$M(t) = 1 - A \sin \omega t \tag{1}$$

Since the field strength ranges from 0.5 to 1.5, *A* must be ½. Since the period is 9000 years,

$$\omega = \frac{2\pi}{9000} = 6.98 \times 10^{-4} \text{ yr}^{-1}$$

Hence

$$Q(t) = K / (1 - \frac{1}{2} \sin \omega t)^{0.52} \tag{2}$$

where *Q(t)* is the production rate cm_e⁻² s⁻¹ and *K* is a constant of proportionality. *Ralph* introduces the approximation that

$$Q = \sim K(1 + \frac{1}{2} \sin \omega t) \tag{3}$$

The time dependence of the total inventory is then

$$\frac{dI}{dt} = -\lambda I + Q(t) \tag{4}$$

where λ is the radiocarbon decay rate. The solution is

$$I = K \left[\frac{1}{\lambda} \frac{\omega}{4(\lambda^2 + \omega^2)} \cos \omega t + \frac{\lambda}{4(\lambda^2 + \omega^2)} \sin \omega t \right] \tag{5}$$

Note that it has been assumed that the 9000-year sinusoidal variation extends indefinitely into the past.

To express (5) in terms of the current magnetic field strength, *M* = 1 implies $t = 2\pi n / \omega$, and hence $Q_0 = K$. Therefore (5) becomes

$$\lambda \frac{I}{Q_0} = 1 - \frac{\lambda \omega}{4(\lambda^2 + \omega^2)} \tag{6a}$$

TABLE 4. Comparison of Radiocarbon and Star Production Rates Under Average Conditions as Determined by *Lal and Peters* [1962] and in This Study

	Lal and Peters	This Study
Star		
Total atmosphere	1.8	1.9
Troposphere	0.6	0.5
Radiocarbon		
Total atmosphere	1.8	1.8
Troposphere	0.8	0.7

Production rates are in units per square centimeter per second averaged over the whole earth.

or perhaps more conveniently,

$$\lambda \frac{I}{Q_0} = 1 - \frac{248 T_{1/2}}{T_{1/2}^2 - 10^6} \tag{6b}$$

where $T_{1/2}$ is the isotopic half-life in years.

The largest departure of the ratio from unity can be seen to occur when $T_{1/2} = 1000$ years, a period of time corresponding half the time to the minimum value of *Q*.

Short term variations. *Lingenfelter* [1963] and *Lingenfelter and Ramaty* [1970] have proposed a relationship of the form

$$Q = A - BR \tag{7a}$$

for the dependence of radiocarbon production on the mean annual sunspot number (Wolf index), where *R* is the Wolf index, allowing an estimate of the effect of solar modulation on the radiocarbon production rate during the last 100 years. By using the calculated dependence of radiocarbon production on solar modulation shown in Table 3 and comparing the Wolf index it is possible to evaluate the agreement between *Lingenfelter's* model and the calculated radiocarbon production rates.

Rao [1972] has synthesized the behavior of the Deep River neutron monitor from 1937 to 1957 from ion chamber data and attached these data to the published counting rates up to 1970, covering 3 complete solar cycles. Conveniently, the mean annual sunspot numbers are also given. Having extracted the Ehmer potential from the counting rate data (via Table 1) and the radiocarbon production rates from the potentials (via

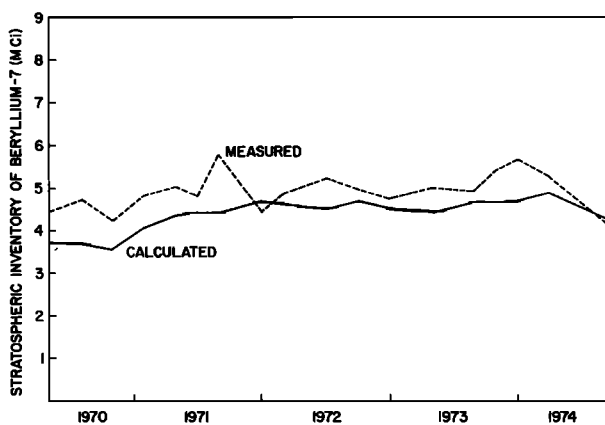


Fig. 3. Measured and calculated stratospheric ⁷Be inventories during 4½ years.

TABLE 5. Calculated Spallation Yields

Isotope	Half-Life	Yield Per Star		R/ST*
		Rudstam	Silberberg-Tsao	
¹⁰ Be	1.50 × 10 ⁶ years	5.07 × 10 ⁻³	1.37 × 10 ⁻²	0.37
²⁶ Al	7.16 × 10 ⁵ years	3.46 × 10 ⁻⁵	2.22 × 10 ⁻⁵	1.60
³⁶ Cl	3.08 × 10 ⁵ years	9.09 × 10 ⁻⁴	4.74 × 10 ⁻⁴	1.90
³² Si	280 years	1.51 × 10 ⁻⁵	3.55 × 10 ⁻⁵	0.43
³ H†	12.3 years	3.35 × 10 ⁻³	1.63 × 10 ⁻²	0.21
²² Na	2.62 years	3.02 × 10 ⁻⁵	1.99 × 10 ⁻⁵	1.50
³⁵ S	87.9 days	2.63 × 10 ⁻⁴	3.17 × 10 ⁻⁴	0.83
⁷ Be	53.6 days	5.37 × 10 ⁻³	3.04 × 10 ⁻²	0.18
³³ P	24.4 days	1.26 × 10 ⁻⁴	1.79 × 10 ⁻⁴	0.70
³² P	14.3 days	2.88 × 10 ⁻⁴	1.86 × 10 ⁻⁴	1.50
²⁸ Mg	21.2 hours	3.30 × 10 ⁻⁶	9.30 × 10 ⁻⁶	0.35
²⁴ Na	15.0 hours	4.46 × 10 ⁻⁵	3.83 × 10 ⁻⁵	1.20
³⁸ S	2.87 hours	3.85 × 10 ⁻⁶	7.75 × 10 ⁻⁶	0.50
³¹ Si	2.62 hours	6.39 × 10 ⁻⁵	8.68 × 10 ⁻⁶	0.74
¹⁸ F	1.83 hours	2.71 × 10 ⁻⁵	1.67 × 10 ⁻⁵	1.60
³⁹ Cl	55.7 min	6.32 × 10 ⁻⁵	5.11 × 10 ⁻⁴	0.12
³⁸ Cl	37.3 min	2.28 × 10 ⁻⁴	3.19 × 10 ⁻⁴	0.71
^{34m} Cl	32.0 min	6.41 × 10 ⁻⁵	2.12 × 10 ⁻⁵	3.00
²⁹ Al	6.56 min	3.40 × 10 ⁻⁵	5.46 × 10 ⁻⁵	0.62
³⁷ S	5.04 min	2.04 × 10 ⁻⁵	2.16 × 10 ⁻⁵	0.94
²⁴ Ne	3.4 min	7.65 × 10 ⁻⁷	2.84 × 10 ⁻⁶	0.27
³⁰ P	2.55 min	4.29 × 10 ⁻⁵	2.29 × 10 ⁻⁵	1.90
²⁸ Al	2.3 min	1.09 × 10 ⁻⁴	8.08 × 10 ⁻⁵	1.30

*Ratio of Rudstam results and Silberberg-Tsao results.

†The production cross section of ³H is not validly given by either of these approaches and was included only because of the importance of the isotope.

Table 3), a least squares fit to the sunspot data yielded

$$Q = 1.937 - 0.00242R \quad (7b)$$

with a standard deviation of 0.098 cm_e⁻² s⁻¹.

The calculated radiocarbon production rates and the predictions of the Lingenfelter model are shown in Figure 6. Agreement is clearly good.

Radiocarbon inventory. It is convenient to treat the short-term (solar) and long-term (geomagnetic) effects on radiocarbon production separately.

Lingenfelter [1963] gives 47.7 as the mean annual sunspot number between 1844 and 1954. This yields 1.822 cm_e⁻² s⁻¹ for the mean production rate during this time. Applying the 5730-

year half-life to the geomagnetic correction (6) yields 1.75 cm_e⁻² s⁻¹ for the current radiocarbon reservoir. This is in excellent agreement with direct estimates of the radiocarbon reservoir based on analyses of the specific activity of ¹⁴C on the earth's surface. Damon *et al.* [1978] give 1.98 cm_e⁻² s⁻¹, Grey [1972] gives 1.8_{-0.04}^{+0.15}, and Suess [1965] gives 1.76. All these estimates lie within or very close to the error bounds on Grey's value. All the above results lie within a range of 12% and are felt to be statistically indistinguishable.

Lingenfelter and Ramaty [1970] have calculated a radiocarbon inventory of 2.2 cm_e⁻² s⁻¹ using experimental neutron flux and density measurements in the literature instead of nucleonic cascade calculations.

TABLE 6. Calculated and Measured Spallation Yields Per Star

Isotope	Calculated Yield	Measured Yield	Percent Deviation*	Coefficient of Variation of Counting Statistics
¹⁰ Be	0.014	0.025†	-44	
³ H	0.016	0.14†		
³⁵ S	3.2 × 10 ⁻⁴	8.6 × 10 ⁻⁴ †	-63	
⁷ Be	0.030	0.045*	-33	
³³ P	1.8 × 10 ⁻⁴	3.8 × 10 ⁻⁴ †	-53	
³² P	1.9 × 10 ⁻⁴	4.6 × 10 ⁻⁴ †	-59	
²⁸ Mg	9.3 × 10 ⁻⁶	1.2 × 10 ⁻⁵ ‡	-22	15
²⁴ Na	3.8 × 10 ⁻⁶	4.4 × 10 ⁻⁶ ‡	-13	18
³⁸ S	7.8 × 10 ⁻⁶	2.9 × 10 ⁻⁵ ‡	-73	20
¹⁸ F	1.7 × 10 ⁻⁵	8.1 × 10 ⁻⁶ ‡	110	36
³⁸ Cl	5.1 × 10 ⁻⁴	1.1 × 10 ⁻³ ‡	-54	5
³⁸ Cl	3.2 × 10 ⁻⁴	7.0 × 10 ⁻⁴ ‡	-54	10
^{34m} Cl	2.1 × 10 ⁻⁵	7.7 × 10 ⁻⁵ ‡	-73	13

*Percent deviation = [(calculated - measured)/measured] × 100.

†Lal and Peters [1967].

‡Inferred from Young *et al.* [1970].

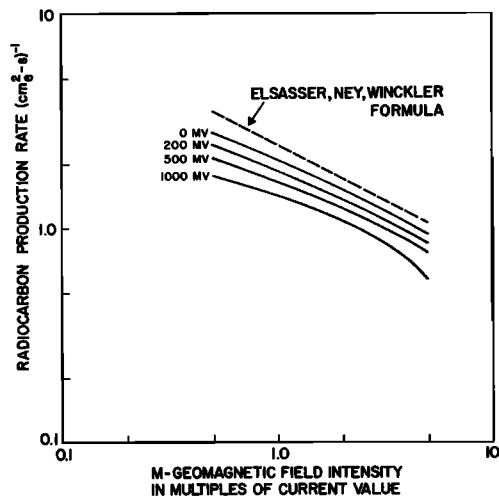


Fig. 4. Worldwide radiocarbon production as a function of M , the geomagnetic field strength in units of the current value, compared with the geomagnetic dependence given by the Elsasser, Ney, and Winckler formula.

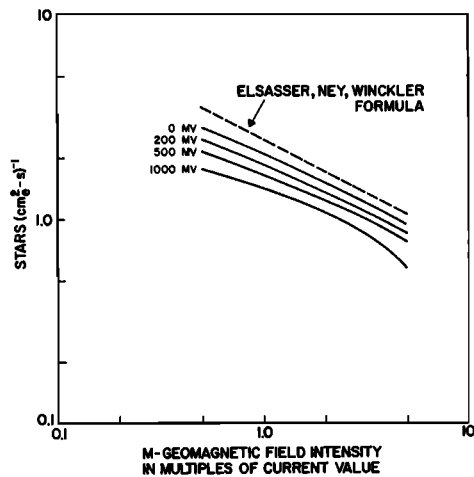


Fig. 5. Worldwide star production as a function of M , the geomagnetic field strength in units of the current value, compared with the geomagnetic dependence given by the Elsasser, Ney, and Winckler formula.

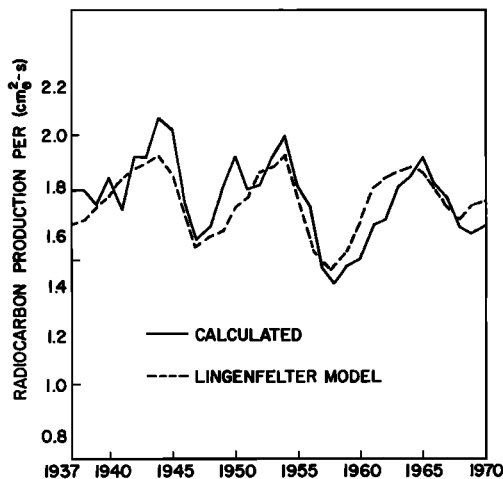


Fig. 6. Worldwide radiocarbon production compared with the Lingenfelter model during solar cycles 19, 20, and 21.

TABLE 7. Comparison of Recent Radiocarbon Production Calculations

Year	<i>Light et al.</i> [1973]	<i>Merker</i> [1970]	This Study
1964	2.42	2.15	1.83
1965	2.58		1.91
1966	2.39		1.80
1967	2.10		1.75
1968	2.03		1.63
1969	1.93	1.86	1.60
1970	1.90		1.63

Values are in units per square centimeter per second averaged over the whole earth.

Two recent calculations of radiocarbon production, those of *Merker* [1970] and *Light et al.* [1973], are compared with the results of this study in Table 7. Both are higher than these results, by 16 and 25%, respectively.

COSMOGENIC ISOTOPE INVENTORY

It is possible on the basis of the foregoing to compile an average inventory of cosmogenic isotopes in the environment. This is shown in Table 8, accounting for the geomagnetic correction and solar modulation effect correction. Spallation yields were the Silberberg-Tsao yields of Table 5 except for tritium, which was taken from the experimental yields of Table 6, and, of course, radiocarbon. The tabular values for materials with half-lives longer than about 1 solar cycle (11 years) represent the total amount actually in the environment. The inventories of materials with shorter lifetimes vary rapidly with time (see, for instance, the ⁷Be concentrations in Figure 3), and the table entries merely represent the average inventory.

CONCLUSION

This paper provides calculated cosmogenic isotope data as a function of geomagnetic field strength and solar modulation, along with spallation yield values based on the recent formula-

TABLE 8. Cosmogenic Isotope Inventory

Isotope	Half-Life	Inventory, cm ₂ -s ⁻¹	Inventory, MCi
¹⁰ Be	1.5 × 10 ⁶ years	2.51 × 10 ⁻²	3.5
²⁶ Al	7.16 × 10 ⁵ years	4.06 × 10 ⁻⁵	0.0056
³⁶ Cl	3.08 × 10 ⁵ years	8.66 × 10 ⁻⁴	0.12
¹⁴ C	5730 years	1.75	241
³ H	280 years	0.255	35
²² Na	2.62 years	3.64 × 10 ⁻⁵	0.0050
³⁵ S	8.79 days	5.80 × 10 ⁻⁴	0.080
⁷ Be	53.6 days	5.56 × 10 ⁻²	7.7
³² P	24.4 days	3.27 × 10 ⁻⁴	0.045
³² P	14.3 days	3.40 × 10 ⁻⁴	0.047
²⁸ Mg	2.12 days	1.70 × 10 ⁻⁵	0.0023
²⁴ Na	15.0 hours	7.00 × 10 ⁻⁵	0.0097
³⁸ S	2.87 hours	1.42 × 10 ⁻⁵	0.0020
³¹ S	2.62 hours	1.59 × 10 ⁻⁴	0.022
¹⁸ F	1.83 hours	3.05 × 10 ⁻⁵	0.0042
³⁹ Cl	55.7 min	9.35 × 10 ⁻⁴	0.13
³⁶ Cl	37.3 min	5.83 × 10 ⁻⁴	0.080
^{34m} Cl	32.0 min	3.88 × 10 ⁻⁵	0.0054
²⁹ Al	65.6 min	99.9 × 10 ⁻⁵	0.0014
³⁷ S	5.04 min	3.95 × 10 ⁻⁵	0.0055
²⁴ Ne	3.4 min	5.19 × 10 ⁻⁶	7.2 × 10 ⁻⁴
³⁰ P	2.55 min	4.19 × 10 ⁻⁵	0.0058
²⁸ Al	2.3 min	1.48 × 10 ⁻⁴	0.020
Total			286

tion of Silberberg and Tsao [1973a, b]. On this basis, the stratospheric inventory of ${}^7\text{Be}$ was calculated as a function of time. Good agreement with experiment was obtained. The Elsasser et al. [1956] formula and the Lingenfelter [1963] sunspot model were evaluated by comparison with the results of this study and were validated. The effects of short-term solar modulation and long-term changes in geomagnetic field strength were taken into account in the calculation of radiocarbon and other radioisotopic reservoirs.

In particular, the measured radiocarbon reservoir was found to agree well with the calculated value. Earlier calculations of radiocarbon production were considerably higher and posed a problem in explaining the actual quantities found [Grey, 1974].

Acknowledgments. The author wishes to acknowledge the advice and encouragement of his colleagues Gail de Planque and Wayne Lowder of this laboratory and Ann Wintle of Simon Fraser University in British Columbia, who pointed out the work of Barbetti et al.

The Editor thanks J. Lerman, P. Damon, R. Sternberg, and another referee for their assistance in evaluating this paper.

REFERENCES

- Armstrong, T. W., K. C. Chandler, and J. Barish, Calculations of neutron flux spectra induced in the earth's atmosphere by galactic cosmic rays, *J. Geophys. Res.*, **78**, 2715, 1973.
- Barashenkov, V. S., K. K. Gudima, and V. D. Toneev, Energy dependence of nuclear cross sections for nucleons at energies above 50 MeV (in Russian), *Dubna Rep. P2-4183*, Joint Inst. for Nucl. Res., Moscow, 1968.
- Barbetti, M., The Lake Mungo geomagnetic excursion, *Phil. Trans. Roy. Soc. London Ser. A*, **281**, 515, 1976.
- Benioff, P. A., Cosmic-ray production rate and mean removal time of beryllium-7 from the atmosphere, *Phys. Rev.*, **104**, 1122, 1956.
- Bland, C. J., and G. Cioni, Geomagnetic cutoff rigidities in non-vertical directions, *Earth Planet. Sci. Lett.*, **4**, 339, 1968.
- Bucha, V., Changes of the earth's magnetic moment and radiocarbon dating, *Nature*, **224**, 681, 1969.
- Bucha, V., Influence of the earth's magnetic field on radiocarbon dating, in *Radiocarbon Variations and Absolute Chronology*, edited by I. U. Olsson, p. 501, John Wiley, New York, 1970.
- Cleghorn, T. F., P. S. Freier, and C. J. Waddington, On the modulation and energy spectrum of highly charged cosmic rays, *Astrophys. Space Sci.*, **14**, 424, 1971.
- Cox, A., Geomagnetic reversals, *Science*, **163**, 237, 1969.
- Damon, P. E., J. C. Lerman, and A. Long, Temporal fluctuations of atmospheric ${}^{14}\text{C}$: Causal factors and implications, *Annu. Rev. Earth Planet. Sci.*, in press, 1978.
- Ehmer, A., On the modulation of the primary spectrum of cosmic rays from solar activity, *Proc. Int. Conf. Cosmic Rays*, **4**, 140, 1960.
- Elsasser, W., E. P. Ney, and J. R. Winckler, Cosmic-ray intensity and geomagnetism, *Nature*, **178**, 1226, 1956.
- Freier, P. S., and C. J. Waddington, Modulation of cosmic rays by an electric field, *Proc. Int. Conf. Cosmic Rays 9th*, **1**, 176, 1965.
- Freier, P. S., and C. J. Waddington, The helium nuclei of the primary cosmic radiation as studied over a solar cycle of activity interpreted in terms of electric field modulation, *Space Sci. Rev.*, **4**, 313, 1966.
- Gleeson, L. J., and W. I. Axford, Cosmic rays in the interplanetary medium, *Astrophys. J.*, **147**, L116, 1967.
- Grey, D., Fluctuations of atmospheric radiocarbon, Ph.D. thesis, Univ. of Ariz., Tucson, 1972. (Also available from Univ. Microfilms, Ann Arbor, Mich., 1974.)
- Hess, W. N., E. H. Canfield, and R. E. Lingenfelter, Cosmic ray demography, *J. Geophys. Res.*, **66**, 665, 1961.
- Kallmann-Bijl, R., L. F. Boyd, H. Lagow, S. M. Poloskov, and W. Priester, in *COSPAR International Reference Atmosphere*, North-Holland, Amsterdam, 1961.
- Kitazawa, K., Intensity of the geomagnetic field in Japan for the past 10,000 years, *J. Geophys. Res.*, **75**, 7403, 1970.
- Krey, P. W., and B. Krajewski, Comparison of atmospheric transport model calculations with observations of radioactive debris, *J. Geophys. Res.*, **75**, 2901, 1970.
- Lal, D., and B. Peters, Cosmic ray produced isotopes and their application to problems in geophysics, in *Progress in Elementary Particle and Cosmic Ray Physics*, vol. 4, edited by J. G. Wilson and S. A. Wouthuysen, pp. 1-74, North-Holland, Amsterdam, 1962.
- Lal, D., and B. Peters, Cosmic ray produced radioactivity on the earth, in *Encyclopedia of Physics*, vol. 46/2, edited by K. Sitte, pp. 551-612, Springer, New York, 1967.
- Light, E. S., M. Merker, H. J. Verschell, R. B. Mendell, and S. A. Korff, Time dependent worldwide distribution of atmospheric neutrons and of their products, 2, Calculation, *J. Geophys. Res.*, **78**, 2741, 1973.
- Lingenfelter, R. E., Production of carbon-14 by cosmic-ray neutrons, *Rev. Geophys.*, **1**, 35, 1963.
- Lingenfelter, R. E., and R. Ramaty, Astrophysical and geophysical variations in C^{14} production, in *Radiocarbon Variations and Absolute Chronology*, edited by I. U. Olsson, p. 513, John Wiley, New York, 1970.
- Merker, M., Solar cycle modulation of fast neutrons in the atmosphere, Ph.D. thesis, New York Univ., New York, 1970. (Also available from Univ. Microfilms, Ann Arbor, Mich., 1971.)
- Newkirk, L. L., Calculations of low-energy neutron flux in the atmosphere by the S_n method, *J. Geophys. Res.*, **68**, 1825, 1963.
- O'Brien, K., Cosmic-ray propagation in the atmosphere, *Nuovo Cimento A*, **3**, 52, 1971.
- O'Brien, K., Propagation of muons underground and the primary cosmic-ray spectrum below 40 TeV, *Phys. Rev. D*, **5**, 597, 1972.
- O'Brien, K., The cosmic ray field at ground level, Natural Radiation Environment II, *USERDA Rep. CONF-72085*, part 1, p. 15, Tech. Info. Serv., U.S. Dep. of Commerce, Springfield, Va., 1975a.
- O'Brien, K., Calculated cosmic-ray pion and proton fluxes at sea level, *J. Phys. A*, **8**, 1530, 1975b.
- O'Brien, K., and G. de P. Burke, Calculated cosmic ray neutron monitor response to solar modulation of galactic cosmic rays, *J. Geophys. Res.*, **78**, 3013, 1973.
- O'Brien, K., H. A. Sandmeier, G. E. Hansen, and J. E. Campbell, Cosmic ray induced neutron background sources and fluxes for geometries of air over water, ground, iron, and aluminum, *J. Geophys. Res.*, **83**, 114, 1978.
- Pal, Y., Cosmic rays, in *Handbook of Physics*, 2nd ed., edited by E. U. Condon and H. Odishaw, pp. 9/272-328, McGraw-Hill, New York, 1967.
- Passow, C., Phenomenologische Theorie zur Berechnung einer Kaskade aus schweren Teilchen (Nukleonenkaskade) in der Materie, *Notiz A 285*, Deut. Electron. Synchrotron, Hamburg, 1962.
- Ralph, E. K., Geophysical implications of radiocarbon measurements, Ph.D. thesis, Univ. of Pa., Philadelphia, 1973. (Also available from Univ. Microfilms, Ann Arbor, Mich., 1974.)
- Rao, U. R., Solar modulation of galactic cosmic radiation, *Space Sci. Rev.*, **12**, 719, 1972.
- Rudstam, G., Systematics of spallation yields, *Z. Naturforsch. A*, **21**, 1027, 1966.
- Shea, M. A., and D. F. Smart, Worldwide trajectory-derived vertical cutoff rigidities and their application to experimental measurements, *J. Geophys. Res.*, **72**, 2021, 1967.
- Silberberg, R., and C. H. Tsao, Partial cross sections in high-energy nuclear reactions, and astrophysical applications, I, Targets with $Z \leq 28$, *Astrophys. J. Suppl. Ser.*, **25**, 315, 1973a.
- Silberberg, R., and C. H. Tsao, Partial cross sections in high-energy nuclear reactions, and astrophysical applications, II, Targets heavier than nickel, *Astrophys. J. Suppl. Ser.*, **25**, 335, 1973b.
- Steljes, J. F., Cosmic ray NM-64 neutron monitor data, XVI-XXIII, May 1970 to December 1972, report, Atomic Energy of Canada, Ltd., Chalk River, Ont., 1973.
- Suess, H. E., Secular variations of the cosmic-ray-produced carbon 14 in the atmosphere and their interpretations, *J. Geophys. Res.*, **70**, 5937, 1965.
- Wilson, M. D., and M. Bercovitch, Cosmic ray NM-64 neutron monitor data, XXIV-XXIX, January 1973 to December 1974, report, National Research Council of Canada, Ottawa, Ont., 1975.
- Yasyulenis, R. Yu, V. Yu. Luyanas, and B. I. Styro, Argon spallation yields of cosmogenic radioisotopes, in *Proceedings of the All-Union Conference on Nuclear Meteorology, Olmink*, translated from Russian by A. Baruch and N. Olaru, Keter Publishing House, Jerusalem, 1974. (Also available from Technical Information Service, U.S. Department of Commerce, Springfield, Va., 1974.)
- Young, J. A., C. W. Thomas, and N. A. Wogman, Cosmogenic radionuclide production rates in argon in the stratosphere, *Nature*, **227**, 160, 1970.

(Received November 21, 1977;
revised August 25, 1978;
accepted September 5, 1978.)